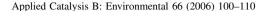


# Available online at www.sciencedirect.com







# Photocatalytic properties of nanosized Bi<sub>2</sub>WO<sub>6</sub> catalysts synthesized via a hydrothermal process

Hongbo Fu, Liwu Zhang, Wenqing Yao, Yongfa Zhu\*

Department of Chemistry, Tsinghua University, Beijing 100084, PR China

Received 20 October 2005; received in revised form 16 February 2006; accepted 17 February 2006

Available online 18 April 2006

#### Abstract

Nanosized  $Bi_2WO_6$  was synthesized by a hydrothermal crystallization process. The as-prepared samples were characterized by X-ray diffraction, Brunauer–Emmet–Teller surface area and porosity measurements, transmission electron microscopy, Raman spectra, and diffuse reflectance spectroscopy. The photoactivities of the as-prepared samples for the rhodamine-B photodegradation were investigated systematically. As a result, the sample prepared at  $180\,^{\circ}\text{C}$  exhibited the highest photochemical activity under visible-light irradiation. The further experiments revealed that the catalyst was active in a wide spectral range. Density functional theory calculations suggested that the visible-light response was due to the transition from the valence band formed by the hybrid orbitals of Bi 6s and O 2p to the conduction band of W 5d. The photoactivity of the catalyst in relationship with the hydrothermal temperature, the crystal and band structure were also discussed in detail. © 2006 Elsevier B.V. All rights reserved.

Keywords: Photocatalytic; Nanosized Bi<sub>2</sub>WO<sub>6</sub>; Hydrothermal synthesis; Rhodamine-B; Visible-light

# 1. Introduction

In the past decades, photocatalytic degradation of harmful pollutants by semiconductors has received considerable attention [1–5]. Outstanding stability and oxidative power make TiO<sub>2</sub> the best semiconductor photocatalyst for environmental remediation. Many persistent organic substances were degraded in TiO<sub>2</sub> suspensions. Even so, slow reaction rate and poor solar efficiency (maximum 5%) have hindered the commercialization of this technology [6–9]. Therefore, in an attempt to eliminate these drawbacks, many studies on modifying surface or bulk properties of TiO<sub>2</sub>, including doping [10–12], codeposition of metals, surface chelation [13], and mixing of two semiconductors [14], have been performed.

On the other hand, many researchers have diverted their attention to exploit new photocatalyst. The outstanding work done by Zou et al. [15] displayed that water splitting for  $H_2$  and  $O_2$  evolution in a stoichiometric amount over  $NiO_x/In_{0.9}Ni_{0.1}$ -  $TaO_4$  photocatalyst under visible-light irradiation. Other mixed oxides, such as  $SrTiO_3$  [16],  $NaTaO_3$  [17],  $ZrO_2$  [18],  $K_4Nb_6O_{17}$  [19],  $Ta_2O_5$  [20],  $BaTi_4O_9$  [21], and  $CaIn_2O_4$ 

[22], have been reported to show high activities. However, only a few studies have been made so far with the aim of environmental clean-up [22].

Nanostructured tungstate materials, such as CdWO<sub>4</sub>, ZnWO<sub>4</sub>, and BaWO<sub>4</sub>, have aroused much interest because of their potential application in various fields, such as in photoluminescence, microwave applications, optical fibers, scintillator materials, and catalysis [23,24]. Due to their unique combination of physical and chemical properties, in terms of molecular and electronic versatility, reactivity, and stability, it is reasonable to believe they may be a promising class of photocatalysts. As expected, Kudo and Hijii [25] have demonstrated photocatalytic O<sub>2</sub> evolution over Bi<sub>2</sub>WO<sub>6</sub> from AgNO<sub>3</sub> solution. More recently, Zou et al. [26] have reported that Bi<sub>2</sub>WO<sub>6</sub> showed not only the activity for photocatalytic O<sub>2</sub> evolution from H<sub>2</sub>O, but also the activity of mineralizing both CHCl<sub>3</sub> and CH<sub>3</sub>CHO under visible-light irradiation. Therefore, the photocatalyst with a strong oxidizing potential could be postulated. However, up to date, we have the dearth of information about the photophysical and photochemical properties of this material. There is an urgent need to observe this photocatalyst systematically.

Recently, many studies have been reported on the preparation and characterization of various nanosized semiconductors. The

<sup>\*</sup> Corresponding author. Tel.: +86 10 6278 3586; fax: +86 10 6278 7601. E-mail address: zhuyf@mail.tsinghua.edu.cn (Y. Zhu).

nanoparticles exhibit special photochemical characteristics [8]. In particular, the band gap of nanoparticles increases with the decrease of the size, resulting in a stronger photocatalytic power. Other important properties such as optical and physical absorption and luminescence emission also undergo drastic changes [24].

In a previous study [27], we have successfully synthesized Bi<sub>2</sub>WO<sub>6</sub> nanoplates by a simple hydrothermal process, and a detailed growth mechanism of Bi<sub>2</sub>WO<sub>6</sub> nanoplates was also clarified. In the present study, to further understand photocatalytic properties of nanostructured Bi<sub>2</sub>WO<sub>6</sub> catalyst, Bi<sub>2</sub>WO<sub>6</sub> catalysts were firstly prepared via the hydrothermal synthesis at different temperature. Bulk and surface characterizations of the powders were carried out by means of X-ray diffractometry (XRD), Brunauer–Emmet–Teller (BET) specific surface areas and porosity measurements, transmission electron microscopy (TEM), laser Raman spectra (LRS), and diffuse reflectance (DR) spectroscopy. The energy band dispersion diagram and density of state (DOS) were obtained by the planewave-density function theory (DFT) calculation. The photoactivities of the as-prepared samples for the rhodamine-B (RhB) photodegradation were systematically investigated. We expected to provide useful information for a greater understanding of the Bi<sub>2</sub>WO<sub>6</sub> photocatalysis from the mechanistic and kinetic viewpoints.

# 2. Experimental

# 2.1. Catalyst preparation

 $Bi_2WO_6$  was prepared via the hydrothermal synthesis according to the previous literature [24,27]. In a typical synthesis procedure, 0.485 g  $Bi(NO_3)_3 \cdot 5H_2O$ , 0.125  $H_2WO_4$  and 0.28 g KOH were added to 9 mL deionized water with magnetic stirring. A series of the reaction mixtures were sealed in a Teflon-lined stainless steel autoclave and heated in the temperature range 120–200° C under autogenous pressure for 24 h. After cooling, the product was filtered, washed and dried at ambient temperature. All chemicals were reagent grade quality and used without further purification. Deionized and doubly distilled water were used throughout this study.  $TiO_{2-x}N_x$ , known for its good photocatalytic activity in decomposition of the pollutants under visible-light irradiation, was also prepared as a reference [10].

# 2.2. Sample characterization

The particle sizes have been determined using a JEOL JEM-1200EX TEM. Specific surface areas were determined in a Flow Sorb 2300 apparatus (Micromeritics) using a single-point BET method. Porosity was monitored using a Sorptomatic 1900 Carlo Erba Instrument from the nitrogen adsorption-desorption isotherms obtained at  $-196^{\circ}$  C. XRD patterns of the powders were recorded at room temperature with a Bruker D8 Advance XRD with Cu K $\alpha$  radiation. UV–vis DR spectra were obtained using a Hitachi U-3010 spectroscopy. LRS were obtained using a Renishaw RM2000 spectrometer equipped with notch filter

and a CCD detector. Total organic carbon (TOC) was measured with a Tekmar Dohrmann Apollo 9000 TOC analyzer.  $NH_4^+$  and  $NO_3^-$  ions were analyzed with a Shimadzu LC-10AS ion chromatograph. The ratio of Bi/W in the sample was determined with a sequential X-ray fluorescence spectrometer (XRF-1700, Shimapzu).

# 2.3. Photochemical experiments

The photocatalytic activities of the samples were evaluated by the RhB decomposition under UV and visible-light irradiation. UV light was obtained by a 12 W Hg lamp ( $\lambda = 254$  nm, the Institute of Electric Light Sources, Beijing) and the average light intensity was 50  $\mu$ W cm<sup>-2</sup>. In the case of visible-light irradiation, a 500 W xenon lamp ( $\lambda > 290$  nm, the Institute of Electric Light Sources, Beijing) was focused through a window. A 420 or 490 nm cutoff filter was placed onto the window face of the cell to ensure the desired irradiation condition. The average light intensity was 40 or 30 mW cm<sup>-2</sup>, respectively. The radiant flux was measured with a power meter (the Institute of Electric Light Sources, Beijing).

Aqueous suspensions (usually 100 mL) of RhB ( $1 \times 10^{-5}$  M) and Bi<sub>2</sub>WO<sub>6</sub> powder (0.5 g L<sup>-1</sup>) were placed in a vessel. Prior to irradiation, the suspensions were magnetically stirred in the dark for ca. 30 min to ensure the adsorption/desorption equilibrium. At given time intervals, 3 mL aliquots were sampled, and centrifugated to remove the particles. The filtrates were analyzed by recording the variations of the absorption band maximum (553 nm) in the UV–vis spectrum of RhB using a Hitachi U-3010 spectrophotometer.

#### 3. Results

#### 3.1. Sample characterization

The morphologies and microstructures of the as-prepared samples were firstly investigated with TEM. The results are shown in Fig. 1. The morphologies and dimensions of the samples are strongly dependent on the hydrothermal temperature. Fig. 1A shows TEM micrograph of the sample prepared at 120° C, nanosized Bi<sub>2</sub>WO<sub>6</sub> crystals display mainly thin sheetshaped morphology and the border lengths of the thin sheets are a few hundreds of nanometer. As the hydrothermal temperature goes up to 140° C, the mixtures of sphere- and sheet-shaped crystals can be seen (Fig. 1B). The crystallite size is several dozens of nanometers. With the increase of the hydrothermal temperature to 160° C, the homogenous sphere-shaped morphologies can be seen. The sizes of these crystals are in the scope of 20-50 nm (Fig. 1C). For the higher-temperature reaction, such as 180 and 200° C, the sheet-shaped crystals are regained. The samples hold the large primary sheets and smaller secondary ones. The close-folded agglomerations of the irregular sheets are clearly seen (Fig. 1D and E).

The surface textural properties of the as-prepared samples were assessed by nitrogen adsorption measurements at  $-196^{\circ}$  C. Fig. 2 shows nitrogen adsorption isotherms and pore size distributions. The curves are similar, irrespective of the

# Download English Version:

# https://daneshyari.com/en/article/49151

Download Persian Version:

https://daneshyari.com/article/49151

Daneshyari.com